



The effect of intramolecular quantum modes on free energy relationships for electron transfer reactions

Ulstrup, Jens; Jortner, Joshua

Published in:
Journal of Chemical Physics

Link to article, DOI:
[10.1063/1.431152](https://doi.org/10.1063/1.431152)

Publication date:
1975

Document Version
Publisher's PDF, also known as Version of record

[Link back to DTU Orbit](#)

Citation (APA):
Ulstrup, J., & Jortner, J. (1975). The effect of intramolecular quantum modes on free energy relationships for electron transfer reactions. *Journal of Chemical Physics*, 63(10), 4358-4368. <https://doi.org/10.1063/1.431152>

General rights

Copyright and moral rights for the publications made accessible in the public portal are retained by the authors and/or other copyright owners and it is a condition of accessing publications that users recognise and abide by the legal requirements associated with these rights.

- Users may download and print one copy of any publication from the public portal for the purpose of private study or research.
- You may not further distribute the material or use it for any profit-making activity or commercial gain
- You may freely distribute the URL identifying the publication in the public portal

If you believe that this document breaches copyright please contact us providing details, and we will remove access to the work immediately and investigate your claim.

The effect of intramolecular quantum modes on free energy relationships for electron transfer reactions

Jens Ulstrup

Chemistry Department A, Building 207, The Technical University of Denmark, 2800 Lyngby, Denmark

Joshua Jortner

Chemistry Department IV, H.C. Ørsted Institute, University of Copenhagen, Universitetsparken 5, 2100 Copenhagen Ø, Denmark

and Department of Chemistry, Tel Aviv University, Tel Aviv, Israel*

(Received 16 May 1975)

A general quantum mechanical description of exothermic electron transfer reactions is formulated by treating such reactions as the nonradiative decay of a "supermolecule" consisting of the electron donor, the electron acceptor, and the polar solvent. In particular, the role of the high-frequency intramolecular degrees of freedom on the free energy relationship for series of closely related reactions was investigated for various model systems involving displacement of potential energy surfaces, frequency shift, and anharmonicity effects. The free energy plots are generally found to pass through a maximum and to be asymmetric with a slower decrease in the transition probability with increasing energy of reaction. For high-frequency intramolecular modes this provides a rationalization of the experimental observation of "activationless" regions. Isotope effects are discussed as also are the oscillatory free energy relationships, predicted for low temperatures and high frequencies, and which are analogous to the vibrational structure in optical transitions.

I. INTRODUCTION

It is possible to provide a general conceptual framework for any chemical reaction in terms of the decay of a metastable state, i. e., a resonance or a set of resonances, and to evaluate the time evolution of the system to obtain the branching into product channels. Such a general approach has already been applied to photophysical processes in excited electronic states, such as electronic relaxation¹ and molecular photofragmentation,² unimolecular decomposition reactions,³ and thermal electron transfer processes in solution.⁴ In the latter case, outer sphere electron transfer reactions can be conceptualized in terms of a decay process between the vibronic levels

$$|av\rangle = \Psi_a \chi_{av}(\mathbf{Q}) \quad (\text{I. 1})$$

and

$$|bw\rangle = \Psi_b \chi_{bw}(\mathbf{Q}), \quad (\text{I. 1}')$$

which correspond to two different electronic states Ψ_a and Ψ_b , characterized by the nuclear wavefunctions $\chi_a(\mathbf{Q})$ and $\chi_b(\mathbf{Q})$, respectively. \mathbf{Q} denotes all the nuclear coordinates of the system. Provided that it is sufficient to consider a two electronic level system, disregarding off-resonance coupling with other electronic states, the transition probability W_{av} for the electron transfer (ET) process $|av\rangle \rightarrow \{|bw\rangle\}$ can be expressed by first order perturbation theory⁵

$$W_{av} = \frac{2\pi}{\hbar} |V(R)|^2 \sum_w |\langle \chi_{av} | \chi_{bw} \rangle|^2 \delta(E_{av} - E_{bw}), \quad (\text{I. 2})$$

where $V(R)$ is the electron exchange matrix element between the electron donor and acceptor, separated by the distance R , and E_{av} and E_{bw} are the (zero order) energies of the vibronic levels $|av\rangle$ and $|bw\rangle$, respectively. When interference effects between resonances can be disregarded, the reaction is nonadiabatic, and

the thermally averaged ET probability W_a from the initial manifold $\{|av\rangle\}$ to the final manifold $\{|bw\rangle\}$ is

$$W_a = Z^{-1} \sum_v \exp(-\beta E_{av}) W_{av}, \quad (\text{I. 3})$$

where

$$Z = \sum_v \exp(-\beta E_{av}) \quad \text{and} \quad \beta = (k_B T)^{-1}.$$

W_a depends explicitly on the separation R via $V(R)$. The bimolecular ET rate constant, k , can be approximated in the form

$$k = \int_{\bar{R}}^{\infty} d^3R \exp[-\beta U(R)] W_a(R), \quad (\text{I. 4})$$

where \bar{R} is the minimum (outer sphere) contact radius of the electron donor and the electron acceptor (in the initial state $|a\rangle$), characterized by the charges $Z_1 e$ and $Z_2 e$, respectively, while $U(R) = Z_1 Z_2 e^2 / D_{\text{eff}} R$ —with D_{eff} being a (loosely defined) effective dielectric constant—represents the donor-acceptor interaction potential.

From Eqs. (I. 3) and (I. 4), we obtain

$$k = AB, \quad (\text{I. 5})$$

where

$$A = (2\pi/\hbar Z) \sum_v \sum_w \exp(-\beta E_{av}) |\langle \chi_{av} | \chi_{bw} \rangle|^2 \delta(E_{av} - E_{bw}) \quad (\text{I. 6})$$

and

$$B = \int_{\bar{R}}^{\infty} |V(R)|^2 \exp[-\beta U(R)] d^3R. \quad (\text{I. 7})$$

Thus, the rate constant can be recast in terms of a product of an electronic contribution B and a term A , which is determined by the nuclear configuration. Both terms depend on the temperature, and the activation energy E_A , for the ET process is

$$E_A = -d(\ln k)/d\beta = \bar{E}_A - d(\ln B)/d\beta, \quad (\text{I. 8})$$

where

$$\bar{E}_A = d(\ln A)/d\beta.$$

An estimate of the magnitude of the electronic term may be obtained⁶ by maximizing the integral (I. 7), that is, taking the integral at $R = R_m$, where its value is a maximum in the range^{4,6} $R > \bar{R}$, so that

$$B \approx |V(R_m)|^2 |R_m^3/3| \exp(-\beta Z_1 Z_2 e^2/D_{\text{eff}} R_m). \quad (\text{I. 7}')$$

The contribution of this term to E_A is then approximately $Z_1 Z_2 e^2/D_{\text{eff}} R_m$, which in polar solvents can be expected to be of the order 2–5 kcal mol⁻¹. When studying the effects of nuclear modes on a given class of “closely related” ET reactions, we can consider the B term to be approximately constant and then refrain from evaluating it. We shall therefore only consider the nuclear term A , i. e., the transition probability normalized by the electronic matrix element.

Equations (I. 3)–(I. 7) constitute a complete theory of nonadiabatic ET, which bears a formal analogy to the calculations of multiphonon electronic and vibrational molecular relaxation processes,¹ nonradiative electron capture, and thermal ionization of impurity centers in solids.^{5a} Furthermore, both the physical and the technical aspects of this quantum mechanical approach practically coincide with Holstein's treatment of the mobility of small polarons^{5b} in the nonadiabatic limit. In all the cases mentioned above, the nonradiative transition probability is determined by a generalized line shape function, which in turn is determined by Franck-Condon vibrational overlap factors between the nuclear wavefunctions, which correspond to the electronic configurations. The expressions for the ET are general, involving all nuclear vibrational modes. The problem is reduced to the specification of the potential energy surfaces, and to the evaluation of the composite density of states at zero energy, weighted by the vibrational overlap factors.

In the following we shall consider ET processes in solution, where the reactants can be either solvated ions or large organic molecules (or organic radical ions). We are interested in the ET probability between two electronic configurations of a “supermolecule,” which consists of the donor-acceptor pair and the entire solvent. The molecular structural aspects of the problem will be incorporated for the electron donor and acceptor centers, whereas the medium outside the organic molecule or the first coordination shell of the solvated ion will be taken as a continuous dielectric. It is then convenient to separate the vibrational modes of the system into two categories:

(a) discrete, high-frequency modes characterized by the nuclear coordinates Q_c and the vibrational frequencies ω_c . These modes do not necessarily have the same equilibrium configurations nor the same frequencies in the two electronic states. Furthermore, these modes are not necessarily adequately represented (for the purpose of calculating A) within the framework of the harmonic approximation, and anharmonicity effects

may be important in determining the ET rate. The high-frequency modes correspond either to metal-ligand vibrations in the first coordination layer of the solvated ions, having $\hbar\omega_c \approx 300\text{--}500\text{ cm}^{-1}$, or to the C-C ($\hbar\omega_c \approx 1000\text{--}1500\text{ cm}^{-1}$) and C-H ($\hbar\omega_c \approx 3000\text{ cm}^{-1}$) modes of organic molecules. Thus, at room temperature, $\hbar\omega_c > k_B T$, and the modes can be adequately classified as quantum modes of the physical system.

(b) low frequency modes of the outer medium, which are characterized by the normal modes q_κ and the corresponding frequencies ω_κ . These are the optical phonon modes of the system and can be adequately described in the harmonic approximation and reasonably well approximated neglecting frequency dispersion effects. The weighted average frequency of these modes is⁷ $\hbar\langle\omega_\kappa\rangle \approx 1\text{ cm}^{-1}$, so that under most experimental conditions $k_B T \gg \hbar\langle\omega_\kappa\rangle$; these modes can then be treated within the framework of the classical approximation, and they will therefore be referred to as the classical modes of the system.

When the equilibrium nuclear configuration and the frequencies of the quantum modes are identical in the initial and final states, the structural aspects of the problem can be disregarded, and the transfer probability is determined by the classical modes only. Levich and Dogonadze have shown^{6,8} how the quantum mechanical treatment for this case results in the well known Gaussian line shape

$$A = (\pi/\hbar^2 E_s k_B T)^{1/2} \exp[-\beta(\Delta E - E_s)^2/4E_s], \quad (\text{I. 9})$$

where ΔE is the energy gap between the minimum of the initial and final potential surfaces. At finite temperatures ΔE corresponds to the free energy of reaction for the ET process. E_s is the solvent reorganization energy, resulting from the response of the outer medium to the change in the charge distribution between the initial and final states. Equation (I. 9) was originally derived by Marcus,⁹ using a purely classical approach, and it gives a simple quadratic free energy relationship

$$\bar{E}_A \approx (\Delta E - E_s)^2/4E_s, \quad (\text{I. 10})$$

which is found to be well obeyed for a number of systems for which $\Delta E < 0$, and $|\Delta E| \ll E_s$.^{10,11}

When configurational changes within the nuclear structure of the reactants are appreciable, the influence of quantum modes will be manifested via the following effects:

(1) The experimental activation energy will be higher than that obtained from Eq. (I. 10) with E_s calculated from Marcus' relation⁹ for the changes in the charging energy in rigid conductors in a dielectric, including corrections for reduction of polarization effects in the space occupied by the reactants.^{12,13} Marcus has provided an extension of his classical treatment to account for this effect,¹⁴ and semiclassical or quantum treatment of the configurational changes of intramolecular modes have also recently been incorporated by Voro-tyntsev, Dogonadze, and Kuznetsov^{15,16} and by Kestner, Logan, and Jortner⁴ for outer sphere ET, by Dogonadze, Ulstrup, and Kharkats¹⁷ for inner sphere ET, and by

German and Dogonadze^{18,19} for ligand substitution reactions, in which a charge redistribution also occurs, and quite extensive comparisons with experimental data have been made.

(2) The activation energy should exhibit a marked temperature dependence. The theory of this effect was worked out by Kestner *et al.*⁴ and by Schmickler,²⁰ but so far no experimental data pertaining to this point are available.

(3) The free energy relation (I. 10) should be modified to include the role of quantum modes. It could be argued that the solvent reorganization energy E_s in Eq. (I. 10) should be replaced by a medium reorganization energy E_M including contributions from both classical and quantum modes, so that $E_M > E_s$. For strongly exothermic reactions when $\Delta E \gg 0$, the activation energy is then expected to be reduced by the effect of the quantum modes. This would be correct only when $k_B T \gg \hbar \omega_c$, and the quantum modes could be treated classically. However, under real physical conditions when $\hbar \omega_c > k_B T$ this formulation has to be grossly modified. In this context, Efrima and Bixon have recently suggested²¹ that vibrational excitation of quantum modes may result in an activationless ET process for strongly exothermic reactions. A similar effect was proposed by Vorotyntsev, Dogonadze, and Kuznetsov.^{15,16} In an experimental study, Rehm and Weller have reported²² that in the fluorescence quenching of large organic molecules in solution, which occurs by ET, the rate constant assumes a maximum value and is independent of ΔE for strongly exothermic reactions ($10 \text{ kcal mol}^{-1} \leq \Delta E \leq 60 \text{ kcal mol}^{-1}$). Fischer²³ and Van Duyne²⁴ have recently studied a number of radical ion recombination reactions involving organic and inorganic systems. It was found that part of the over-all annihilation rate for large free energy changes could be ascribed to an ET reaction channel, for which an almost linear dependence between the free energy of activation and free energy of reaction was found.

Thus, there is at present some evidence for serious deviations from the free energy relationship (I. 10), giving a lowering of the activation energy with ΔE for sufficiently large values of the latter. Provided that ΔE is still not large enough to induce electronic excitations, the detailed role of the quantum modes must therefore be considered. In the present work we utilize a general theory of nonadiabatic ET processes involving both quantum and classical modes.⁴ The general line shape function (I. 6) will be recast in terms of a convolution of separate contributions originating from the classical and from quantum modes. Adopting various models for the quantum subsystem we were able to elucidate the role of the quantum modes in modifying the free energy relationships for strongly exothermic ET processes.

II. QUANTUM MODES IN ELECTRON TRANSFER REACTIONS

The potential energy surfaces of the initial state $U_a(\mathbf{Q})$ and final state $U_b(\mathbf{Q})$ are separated into the additive contributions from the intramolecular donor \mathbf{Q}_a^D

or \mathbf{Q}_b^D and acceptor quantum modes \mathbf{Q}_a^A or \mathbf{Q}_b^A and from the solvent modes \mathbf{Q}_a^S and \mathbf{Q}_b^S . The subscripts a and b refer to the appropriate electronic state. Then,

$$\begin{aligned} U_a(\mathbf{Q}) &= f_a^D(\mathbf{Q}_a^D) + f_a^A(\mathbf{Q}_a^A) + g_a^S(\mathbf{Q}_a^S), \\ U_b(\mathbf{Q}) &= f_b^D(\mathbf{Q}_b^D) + f_b^A(\mathbf{Q}_b^A) + g_b^S(\mathbf{Q}_b^S). \end{aligned} \quad (\text{II. 1})$$

The solvent contribution can be recast in the harmonic approximation, neglecting dispersion effects,

$$\begin{aligned} g_a^S(\mathbf{Q}_a^S) &= \hbar \langle \omega_\kappa \rangle \sum_\kappa q_\kappa^2, \\ g_b^S(\mathbf{Q}_b^S) &= g_a^S(\mathbf{Q}_a^S) - \hbar \langle \omega_\kappa \rangle \sum_\kappa q_\kappa \Delta_\kappa + E_s. \end{aligned} \quad (\text{II. 2})$$

The reduced solvent modes are $q_\kappa = (\mu_\kappa \omega_\kappa / \hbar)^{1/2} Q_a^S$ for each mode, and E_s , which appeared at first in equation (I. 10), is

$$E_s = \frac{1}{2} \hbar \langle \omega_\kappa \rangle \sum_\kappa \Delta_\kappa^2. \quad (\text{II. 3})$$

Δ_κ represents the reduced displacements for the solvent coordinate κ between the origins of the two potential surfaces. We now factorize the vibrational wavefunction (I. 1) into the products

$$\begin{aligned} \chi_{av}(\mathbf{Q}_a^D, \mathbf{Q}_a^A, \mathbf{Q}_a^S) &= \chi_a^D(\mathbf{Q}_a^D; \epsilon_a^D) \chi_a^A(\mathbf{Q}_a^A; \epsilon_a^A) \chi_a^S(\mathbf{Q}_a^S; v_\kappa), \\ \chi_{bw}(\mathbf{Q}_b^D, \mathbf{Q}_b^A, \mathbf{Q}_b^S) &= \chi_b^D(\mathbf{Q}_b^D; \epsilon_b^D) \chi_b^A(\mathbf{Q}_b^A; \epsilon_b^A) \chi_b^S(\mathbf{Q}_b^S; w_\kappa), \end{aligned} \quad (\text{II. 4})$$

where χ_i^D , χ_i^A , and χ_i^S ($i = a$ or b) represents the nuclear wavefunction of the donor, the acceptor, and the solvent, respectively. The vibrational energy levels of the donor are labeled by ϵ_i^D , those of the acceptor by ϵ_i^A , and the solvent energy levels are given by $\epsilon_a^S = \sum_\kappa (v_\kappa + \frac{1}{2}) \hbar \langle \omega_\kappa \rangle$, and $\epsilon_b^S = \sum_\kappa (w_\kappa + \frac{1}{2}) \hbar \langle \omega_\kappa \rangle$ in the states a and b , respectively. The total potential energies in the initial and final states are then

$$\begin{aligned} E_{av} &= \epsilon_a^D + \epsilon_a^A + \sum_\kappa (v_\kappa + \frac{1}{2}) \hbar \langle \omega_\kappa \rangle + \Delta E, \\ E_{bw} &= \epsilon_b^D + \epsilon_b^A + \sum_\kappa (w_\kappa + \frac{1}{2}) \hbar \langle \omega_\kappa \rangle. \end{aligned} \quad (\text{II. 5})$$

The nuclear contribution to the ET probability is

$$\begin{aligned} A &= (Z_D Z_A Z_S)^{-1} \sum_{\epsilon_a^D} \sum_{\epsilon_a^A} \sum_{\epsilon_a^S} \sum_{\epsilon_b^D} \sum_{\epsilon_b^A} \sum_{\epsilon_b^S} \exp[-\beta(\epsilon_a^D + \epsilon_a^A + \epsilon_a^S)] \\ &\otimes S_D(\epsilon_a^D, \epsilon_b^D) S_A(\epsilon_a^A, \epsilon_b^A) S_S(\epsilon_a^S, \epsilon_b^S) \\ &\otimes \delta(\epsilon_a^D - \epsilon_b^D + \epsilon_a^A - \epsilon_b^A + \epsilon_a^S - \epsilon_b^S + \Delta E), \end{aligned} \quad (\text{II. 6})$$

where Z_D , Z_A , and Z_S are the partition functions. Also,

$$Z_I = \sum_{\epsilon_i^I} \exp(-\beta \epsilon_i^I) \quad I = D, A, S \quad (\text{II. 7})$$

for the nuclear energy levels. The Franck-Condon vibrational overlap terms between the two electronic states are

$$S_I(\epsilon_a^I, \epsilon_b^I) = |\langle \chi_a^I(\mathbf{Q}_a^I; \epsilon_a^I) | \chi_b^I(\mathbf{Q}_b^I; \epsilon_b^I) \rangle|^2 \quad I = D, A, S. \quad (\text{II. 8})$$

Equation (II. 6) can be recast in the form

$$A = \int_0^\infty dx F_D(x) F_S(\Delta E - x), \quad (\text{II. 9})$$

where we have defined the auxiliary functions

$$F_Q(x) = (Z_D Z_A)^{-1} \sum_{\epsilon_a^D} \sum_{\epsilon_a^A} \sum_{\epsilon_b^D} \sum_{\epsilon_b^A} \exp[-\beta(\epsilon_a^D + \epsilon_a^A)] \\ \otimes S_D(\epsilon_a^D; \epsilon_b^D) S_A(\epsilon_a^A; \epsilon_b^A) \delta(\epsilon_a^D - \epsilon_b^D + \epsilon_a^A - \epsilon_b^A + x) \quad (\text{II. 10})$$

and

$$F_S(\Delta E - x) = (Z_S)^{-1} \sum_{\epsilon_a^S} \sum_{\epsilon_b^S} \exp(-\beta\epsilon_a^S) S_S(\epsilon_a^S; \epsilon_b^S) \delta(\epsilon_a^S - \epsilon_b^S + x), \quad (\text{II. 11})$$

which correspond to energy-dependent line shape functions, or transition probabilities for the quantum modes (Q) and for the classical solvent modes (S). The line shape function for the low frequency solvent modes can be expressed in the classical approximation (for $\hbar\omega_s \ll k_B T$) as

$$F_S(\Delta E - x) = (\pi/\hbar^2 E_S k_B T)^{1/2} \exp[-\beta(\Delta E - E_S - x)^2/4E_S k_B T] \quad (\text{II. 12})$$

which is a generalization of Eq. (I. 10). Equations (II. 10) and (II. 12) give the final form of the ET probability,

$$A = (\pi/\hbar^2 E_S k_B T)^{1/2} (Z_A Z_D)^{-1} \sum_{\epsilon_a^D} \sum_{\epsilon_a^A} \sum_{\epsilon_b^D} \sum_{\epsilon_b^A} \exp[-\beta(\epsilon_a^D + \epsilon_a^A)] \\ \otimes \exp[-\beta(\Delta E - E_S + \epsilon_a^D - \epsilon_b^D + \epsilon_a^A - \epsilon_b^A)^2/4E_S] \\ \otimes S_D(\epsilon_a^D; \epsilon_b^D) S_A(\epsilon_a^A; \epsilon_b^A). \quad (\text{II. 13})$$

In many systems of physical interest the quantum modes are expected to be "frozen," i. e., $k_B T \ll \hbar\omega_c$ for all the donor and acceptor frequencies of the initial state. In such cases we can set $\epsilon_a^D = \epsilon_a^A = 0$, and Eq. (II. 13) simplifies to

$$A = (\pi/\hbar^2 E_S k_B T)^{1/2} \sum_{\epsilon_b^D} \sum_{\epsilon_b^A} \exp[-\beta(\Delta E - E_S - \epsilon_b^D - \epsilon_b^A)^2/4E_S] \\ \otimes S_D(0, \epsilon_b^D) S_A(0, \epsilon_b^A). \quad (\text{II. 13}')$$

Equation (II. 13) together with Eqs. (I. 5) and (I. 7) provide us with a working theory for nondiabatic ET processes. These general results rest on the harmonic approximation for the classical modes, which is entirely justified. The quantum modes are deconvoluted and otherwise are of a general form. Therefore, such factors as frequency changes, anharmonicity effects, etc. in these modes can be accounted for in the present formalism. Furthermore, Eq. (II. 13) provides a general framework for the quantitative interpretation of the three effects of quantum modes listed previously.

In the following we shall focus attention on the free energy relationships predicted by Eqs. (II. 13) and (II. 13'). In the present theory the nuclear contribution to the ET rate constant is recast in terms of converging sums, in which each term involves products of a Gaussian type function for the classical modes and Franck-Condon vibrational overlap factors for the quantum modes. In view of the voluminous literature available in the field of molecular spectroscopy, concerning the evaluation of the latter terms for a variety of model systems, we can directly proceed to the application of

these results for our problem.

III. FREE ENERGY RELATIONSHIPS FOR MODEL SYSTEMS

The problem of the quantitative determination of the dependence of the ET rate constant on ΔE now reduces to the specification of the nuclear potential surfaces in the initial and in the final state, followed by the evaluation of the Franck-Condon vibrational overlap factors

$$S_{ab}^{DA} \equiv S_D(\epsilon_a^D; \epsilon_b^D) S_A(\epsilon_a^A; \epsilon_b^A) \quad (\text{III. 1})$$

for the quantum modes in Eqs. (II. 11) and (II. 13).

In view of the low frequency of the solvent modes ($\hbar\omega_s \approx 1 \text{ cm}^{-1}$), these modes are always treated classically (in the high temperature limit), as is evident from Eq. (II. 13). Regarding the quantum modes of the system we can consider three cases: (a) the low temperature range, $k_B T \ll \hbar\omega_c$, where the quantum modes are frozen and the "intramolecular" vibrational overlap factor is

$$S_{ab}^{DA} \equiv S_D(0, \epsilon_b^D) S_A(0, \epsilon_b^A); \quad (\text{III. 1}')$$

(b) the intermediate temperature range where $k_B T < \hbar\omega_c$, and where mode-rate excitation of quantum modes prevails. In this range, Eq. (III. 1) has to be utilized in the sums of (II. 13). (c) The high temperature range $k_B T > \hbar\omega_c$, where again Eq. (III. 1) has to be adopted and where in the limit of extremely high temperatures the rate constant reduces to a Gaussian line shape function analogous to Eq. (I. 10), with a modified value of E_S . As we have already noted, from a practical point of view, cases (a) and (b) are of interest *a priori*, and numerical calculations show that case (c) can also be achieved for frequencies for which $\hbar\omega_c$ are only slightly smaller than $k_B T$. We shall now proceed to consider free energy relationships for model systems.

A. Displaced potential surfaces

The simplest model involves a system characterized by displaced harmonic nuclear potential surfaces for the quantum modes $i = 1, 2, \dots, N$, where the frequencies $\hbar\omega_{ci}$ for each mode are identical in the initial and in the final states. The minimum of the potential surfaces are displaced by ΔQ_i^0 for the i th vibrational mode, the corresponding reduced displacement being $\Delta_{ci} = (\mu_i \omega_{ci} / \hbar)^{1/2} \Delta Q_i^0$. The Franck-Condon vibrational overlap factors in the harmonic approximation are well known.^{1,4} The vibrational overlap factors (III. 1) can thus be represented in terms of a product

$$S_{ab}^{DA} = \prod_{i=1}^N S_{ab}^{DA}(v_i, w_i), \quad (\text{III. 1}'')$$

where $S_{ab}^{DA}(v_i, w_i)$ is the square of the vibrational overlap integral for the i th mode, which is characterized by the quantum number v_i in the initial state and w_i in the final state. The sets of initial $\{v_i\}$ and final $\{w_i\}$ vibrational quantum numbers are determined by the relations

$$\sum_{i=1}^N v_i \hbar\omega_{ci} = \epsilon_a^D + \epsilon_a^A \quad \text{and} \quad \sum_{i=1}^N w_i \hbar\omega_{ci} = \epsilon_b^D + \epsilon_b^A + \Delta E.$$

The vibrational overlap factors for the single modes are given by^{1,2,4,25}

$$s_a^{D_A}(v_i, w_i) = e^{-\Delta_{ci}^2/2} \frac{v_i!}{w_i!} (\Delta_{ci}^2/2)^{|w_i-v_i|} [L_{v_i}^{w_i-v_i}(\Delta_{ci}^2/2)]^2, \quad (\text{III. 2})$$

where $L_\alpha^{\beta-\alpha}(x)$ is the Laguerre polynomial. In the low temperature limit for the quantum modes [case (a)],

Eq. (III. 2) reduces to the well known form

$$s_{ab}^{D_A}(0, w_i) = \exp(-\Delta_{ci}^2/2) (\Delta_{ci}^2/2)^{w_i} / w_i!. \quad (\text{III. 3})$$

Calculations of the nonradiative transition probabilities utilizing Eqs. (I. 5), (II. 13), and (III. 2) or (III. 3) can be readily performed by the generating function method^{1,5a}; we shall just quote the pertinent final results. The nuclear contribution A [Eq. (I. 6)] to the rate constant is⁴

$$A = \left(\frac{\pi}{\hbar^2} E_s k_B T \right)^{1/2} \exp\left(-\frac{1}{2} \sum_{i=1}^N \Delta_{ci}^2 \tanh\left(\frac{1}{2} \beta \hbar \omega_{ci}\right)\right) \otimes \sum_{l_1=0}^{\infty} \sum_{k_1=0}^{\infty} \sum_{l_2=0}^{\infty} \sum_{k_2=0}^{\infty} \cdots \sum_{l_N=0}^{\infty} \sum_{k_N=0}^{\infty} \exp\left[-\beta\left(\Delta E - E_s - \sum_{i=1}^N (l_i - k_i) \hbar \omega_{ci}\right)^2 / 4E_s\right] \otimes \prod_{i=1}^N \left[\frac{1}{l_i! k_i!} \left(\frac{\Delta_{ci}^2 \exp(-\beta \hbar \omega_{ci}/2)}{4 \sinh(\beta \hbar \omega_{ci}/2)} \right)^{l_i+k_i} \exp(l_i \beta \hbar \omega_{ci}/2) \right]. \quad (\text{III. 4})$$

This result is valid at all temperatures. At sufficiently low temperatures, when $\beta \hbar \omega_{ci} < 1$ [case (b)], an important limiting form of Eq. (III. 4) is^{4,25}

$$A = (\pi / \hbar^2 E_s k_B T)^{1/2} \exp\left(-\frac{1}{2} \sum_{i=1}^N \Delta_{ci}^2\right) \otimes \sum_{w_1=-\infty}^{\infty} \sum_{w_2=-\infty}^{\infty} \cdots \sum_{w_N=-\infty}^{\infty} \prod_{i=1}^N (|w_i|!)^{-1} (\Delta_{ci}^2/2)^{|w_i|} \otimes \exp\left(-\beta \sum_{i=1}^N (w_i + |w_i|) \hbar \omega_{ci}/2\right) \exp\left(-\beta(\Delta E - E_s - \sum_{i=1}^N w_i \hbar \omega_{ci})^2 / 4E_s\right). \quad (\text{III. 4}')$$

Finally, in the low temperature limit [case (a)] one gets

$$A = (\pi / \hbar^2 E_s k_B T)^{1/2} \exp\left(-\frac{1}{2} \sum_{i=1}^N \Delta_{ci}^2\right) \otimes \sum_{w_1=0}^{\infty} \sum_{w_2=0}^{\infty} \cdots \sum_{w_N=0}^{\infty} \prod_{i=1}^N \frac{(\Delta_{ci}^2)^{w_i}}{w_i!} \exp\left(-\beta(\Delta E - E_s - \sum_{i=1}^N w_i \hbar \omega_{ci})^2 / 4E_s\right). \quad (\text{III. 4}'')$$

It is worthwhile to notice that for the present model system each term in the sum which determines the rate constant is given by a product of a Gaussian function and a member of a Poisson distribution.

We have performed a series of model computer calculations of the relationship between A and ΔE , as given by Eq. (III. 4) and its intermediate temperature limit (III. 4'). The frequencies of the quantum modes were selected in the range $\hbar \omega_{ci} = 200$ – 3000 cm^{-1} . The lower values $\hbar \omega_{ci} = 200$ – 600 cm^{-1} correspond to the vibrational frequencies of the ligands in transition metal complexes, while the range of high frequencies $\hbar \omega_{ci} = 1000$ – 3000 cm^{-1} represent the skeleton and the C–H modes of aromatic hydrocarbons. The (reduced) potential displacement parameters were chosen in the range $\Delta_{ci} = 1$ – 10 . Displacement for quantum modes in outer sphere ET reactions are often quite small ($\Delta_{ci} \approx 1$)^{4,17-19}. In other reactions, e.g., those of some Co(III) complexes,^{11,26} and in particular for proton transfer reactions,²⁵ the displacements may be substantial ($\Delta_{ci} \gtrsim 10$). The medium rearrangement energy was chosen to be^{6,8,9} $E_s = 1 \text{ eV}$. We have used the free energy interval $\Delta = 0$ – 4 eV noting that for higher values of ΔE ($\gtrsim 3 \text{ eV}$, or so) excited electronic states are expected to participate. The temperature range covered was 30–300 K, which for most cases corresponds to the low temperature [case (a)] situation, although for the lowest frequencies and the highest temperatures employed the intermediate temperature limit prevails [case (b)]. In Figs. 1 and 2 we portray the results of such model calculations for a system characterized by a single displaced quantum mode. Inspection of Equation (III. 4) and the numerical calculation reveal that even for the high values of $\hbar \omega_c$ considered herein,

several vibrational levels yield comparable contributions to A , and in the relevant ΔE interval quite high values of the vibrational quantum numbers have to be incorporated (up to $w \approx 10$ for $\hbar \omega_c = 2000 \text{ cm}^{-1}$ and $\Delta_c = 10$). Thus, the effect of vibrational excitation of quantum modes in the ET process is appreciable. The numerical data also reveal the following quantum effects:

(a) In general, a maximum in the free energy relationship is exhibited, which for the classical system is lo-

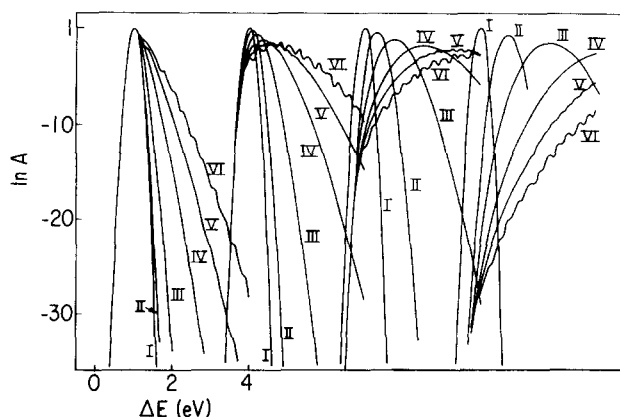


FIG. 1. Free energy plots for displacement of one quantum mode of constant frequency. Low temperature approximation [Eq. (III. 4')], and $T = 30 \text{ K}$. The four families of curves refer to (from left to right) $\Delta_c = 1, 2.5, 5,$ and 7.5 , and the origins of the latter three are shifted by $3 \text{ eV}, 6 \text{ eV},$ and 9 eV along the ΔE axis. Within each family, the Roman numerals refer to different frequencies of the quantum mode: I: classical (i.e., no quantum modes); II: $\hbar \omega_c = 206 \text{ cm}^{-1}$; III: $\hbar \omega_c = 514 \text{ cm}^{-1}$; IV: $\hbar \omega_c = 1029 \text{ cm}^{-1}$; V: $\hbar \omega_c = 1543 \text{ cm}^{-1}$; VI: $\hbar \omega_c = 2058 \text{ cm}^{-1}$.

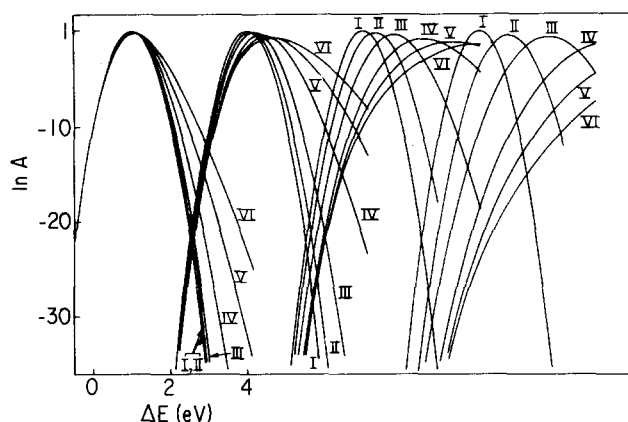


FIG. 2. Free energy plots for displacement of one quantum mode of constant frequency. Finite temperature formula [Eq. (III. 4)], and $T=298^\circ\text{K}$. The four families of curves and the Roman numerals correspond to those of Fig. 1, where the appropriate values of Δ_c and $\hbar\omega_c$ are given.

cated at $\Delta E = E_s$, whereas quantum effects result in a shift of this maximum by roughly $\Delta_c^2 \hbar\omega_c / 2$ towards higher ΔE values.

(b) The free energy relationships are asymmetric about the value of $\Delta E = \Delta E_{\max}$ corresponding to the maximum value, A_{\max} , of A . Incorporation of a quantum mode results in a slower decrease of $\ln A$ with increasing ΔE for $\Delta E \geq E_{\max}$, i. e., beyond the maximum.

(c) At sufficiently low temperatures, an oscillatory dependence of $\ln A$ on ΔE is revealed for high values of $\hbar\omega_c$. We shall show in Sec. IV that this effect is exhibited provided that $2(E_s k_B T)^{1/2} < \hbar\omega_c$ and provided that it is not smeared out by frequency congestion effects, when several modes of different frequencies and finite values of Δ_{c_i} contribute to the ET rate. At higher temperatures these interesting oscillations are smeared out.

(d) Increasing the temperature for constant Δ_c and $\hbar\omega_c$ results in broadening of the ball-shaped curve that represents the free energy relationship; the broadening is roughly proportional to $T^{1/2}$, as is the situation for the classical case, Eq. (I. 9).

(e) For higher frequencies, i. e., $\hbar\omega_c \approx 2000\text{--}3000\text{ cm}^{-1}$, and for intermediate values of $\Delta_c \approx 2\text{--}5$, the free energy relationship at room temperature exhibits a broad flat maximum. Thus, for example, for $\Delta_c = 2.5$ and $\hbar\omega_c \approx 2000\text{ cm}^{-1}$ (Fig. 2) $\ln A$ varies weakly in the range $\Delta E = 1.2\text{--}2.2\text{ eV}$. An activationless region is not predicted for the simple model system which involves a single quantum mode; however, the dependence of A on ΔE is considerably weaker over a broad ΔE range than for a purely classical system. This effect will be most pronounced when high frequency modes prevail, such as in the case of ET involving aromatic hydrocarbons and their radical ions.

(f) Interesting isotope effects are expected to be revealed when the role of quantum modes is important. For $\Delta E < \Delta E_{\max}$, the ET rate constant will increase with decreasing frequency of the quantum modes (i. e., an inverse isotope effect); whereas for $\Delta E > \Delta E_{\max}$, a normal

isotope effect will be exhibited, i. e., the ET rate constant will decrease with decreasing $\hbar\omega_c$.

Further numerical calculations were performed for a model system with two displaced modes, which are characterized either by equal or by different frequencies. These two modes may correspond, for example, to the totally symmetric A_{1g} breathing frequencies of the donor and acceptor in ET reactions involving octahedral complexes. The resulting free energy relationships (Figs. 3 and 4) are qualitatively similar to those obtained for a single displaced mode. However, the asymmetry is more pronounced with increasing number of quantum modes and with increasing $\hbar\omega_{c_i}$ ($i = 1, 2$). We expect that for intermediate values of $\Delta_{c1} \approx \Delta_{c2} \approx 2\text{--}5$, a flat portion of the $\ln A$ vs ΔE curve will be exhibited over quite a broad ΔE range. As expected, the oscillatory behavior revealed at low temperatures for a single quantum mode is largely eroded when two displaced modes with different frequencies are involved.

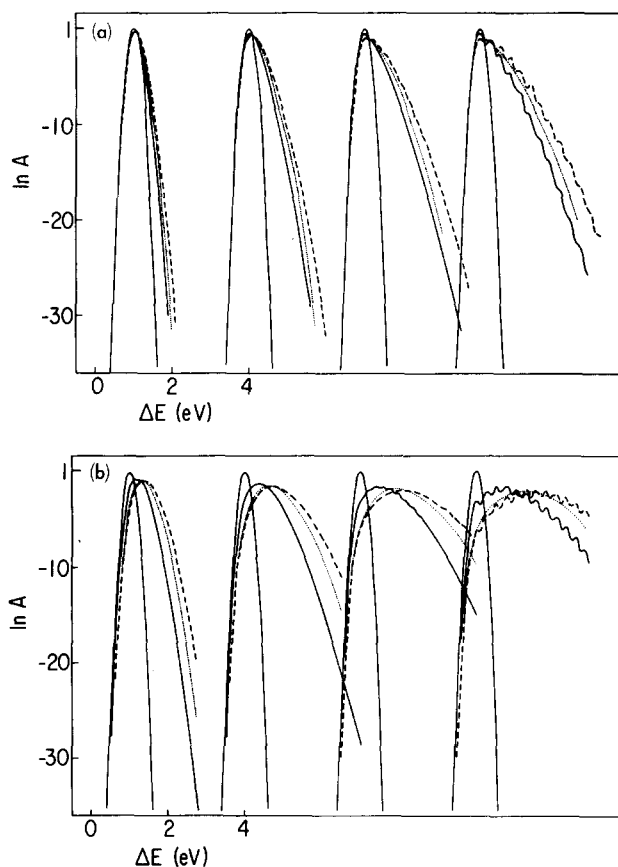


FIG. 3. (a) Free energy plots for displacement of two quantum modes of constant frequencies, ($\Delta_{c1} = \Delta_{c2} = 1$). Low temperature approximation [Eq. (II. 4')], and $T=30^\circ\text{K}$. The four families of curves (from left to right) refer to $\hbar\omega_{c1} = 514\text{ cm}^{-1}$; $\hbar\omega_{c1} = 1029\text{ cm}^{-1}$; $\hbar\omega_{c1} = 1543\text{ cm}^{-1}$; and $\hbar\omega_{c1} = 2058\text{ cm}^{-1}$, and the origins of the latter three are shifted by 3 eV, 6 eV, and 9 eV along the ΔE axis. Within each family, the curves listed in the order of increasing asymmetry are classical; one displaced quantum mode; two displaced quantum modes ($\hbar\omega_{c2} = 0.7 \hbar\omega_{c1}$); and two displaced quantum modes ($\hbar\omega_{c2} = \hbar\omega_{c1}$). (b) Free energy plots for displacement of two quantum modes of constant frequencies ($\Delta_{c1} = \Delta_{c2} = 2.5$). Low temperature approximation [Eq. (III. 4')], and $T=30^\circ\text{K}$. The frequencies and the arrangement of the plots are the same as in Fig. 3(a).

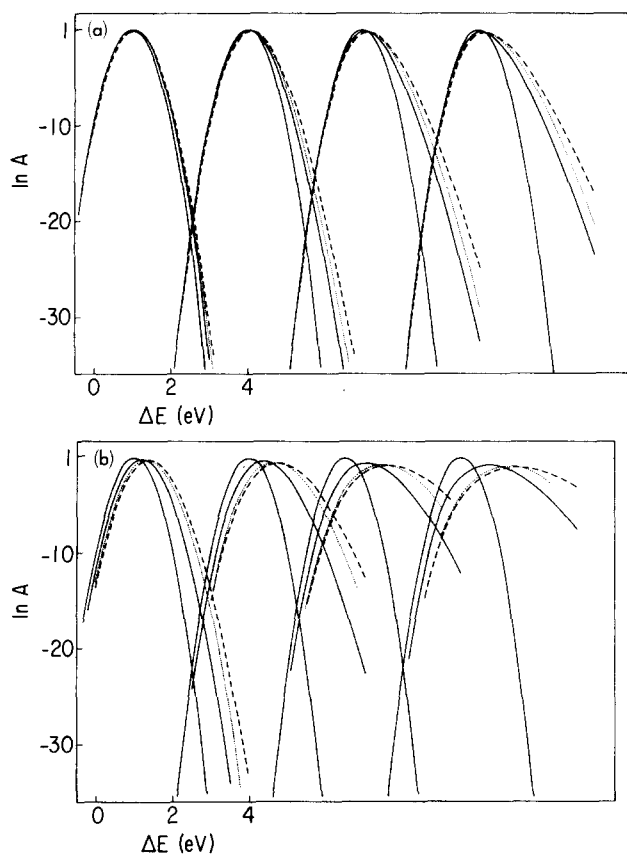


FIG. 4. (a) Free energy plots for displacement of two quantum modes of constant frequencies ($\Delta_{c1} = \Delta_{c2} = 1$). Finite temperature formula [Eq. (III. 4)], and $T = 298^\circ\text{K}$. The frequencies and the arrangement of the plots are the same as in Figs. 3(a) and 3(b). (b) Free energy plots for displacement of two quantum modes of constant frequencies ($\Delta_{c1} = \Delta_{c2} = 2.5$). Finite temperature formula [Eq. (III. 4)], and $T = 298^\circ\text{K}$. The frequencies and the arrangement of the plots are the same as in Figs. 3(a), 3(b), and 4(a).

B. Effects of frequency changes

ET reactions are usually accompanied by changes of the intramolecular vibrational frequencies of the reacting species. Furthermore, these changes are sometimes known experimentally. It is therefore of considerable importance to investigate the effect of frequency changes on the over-all transition probability.

General expressions for the transition probability, including frequency shifts, have been developed by several authors.^{15,16,27,28} However, in most cases the resulting equations are complicated and rather difficult to apply. In what follows we shall use a simpler analysis of the Franck-Condon factors in order to obtain a general form of the free energy relationship for large ΔE .

For a single mode which undergoes both displacement and frequency change, the Franck-Condon factor for transition from the ground vibrational level of the initial state to the w th vibrational level of the final state can be written^{29,30}

$$S_{ab}^{DA}(0, w) = F(0) \left(\frac{1}{2}\xi\right)^w |H_w(ix)|^2 / w! , \quad (\text{III. 5})$$

where

$$F(0) = (1 - \xi^2)^{1/2} \exp(-\Delta_c^2/2) ,$$

$$\xi = (\omega_{ci} - \omega_{cf}) / (\omega_{ci} + \omega_{cf}) ,$$

$$\Delta_c^2/2 = (k^i k^f)^{1/2} (Q_{bo} - Q_{ao})^2 / \hbar(\omega_{cf} + \omega_{ci}) ,$$

$$x = [\Delta_c^2 \omega_{cf} / 2(\omega_{ci} - \omega_{cf})]^{1/2} = [\Delta_c^2(1 - \xi) / 4\xi]^{1/2} .$$

k^i and k^f are the force constants of the particular mode in the initial and final state, respectively, and Q_{ao} and Q_{bo} are the equilibrium values of the coordinate (no change in normal modes is assumed in the analysis). ω_{ci} and ω_{cf} are the frequencies in the initial and final state, and $H_w(ix)$ is the Hermite polynomial of an imaginary argument, i. e.,

$$H_w(ix) = (-1)^w w! \sum_{r=0}^{w/2} [(-1)^r (2ix)^{w-2r} / (w-2r)! r!] . \quad (\text{III. 6})$$

It can be shown that for $\xi \rightarrow 0$, corresponding to a pure displacement with no frequency change, Eq. (III. 5) takes the form previously obtained, i. e., Eq. (III. 3):

$$S_{ab}^{DA}(0, w) = \exp(\Delta_c^2/2) (\Delta_c^2/2)^w / w! . \quad (\text{III. 7})$$

For a purely distorted mode (i. e., involving frequency changes) with no displacement, Eq. (III. 5) takes the form

$$S_{ab}^{DA}(0, w) = (1 - \xi^2)^{1/2} \xi^w \frac{1 \times 3 \times 5 \cdots (w-1)}{2 \times 4 \times 6 \cdots w} \quad \text{for } w \text{ even} \quad (\text{III. 8})$$

$$S_{ab}^{DA}(0, w) = 0 \quad \text{for } w \text{ odd} .$$

Using this result, the ET probability for a process involving distortion in a single mode, but no displacement, becomes

$$A = (\pi / \hbar^2 E_S k_B T)^{1/2} (1 - \xi^2)^{1/2} \sum_{w=0}^{\infty} \xi^w \frac{1 \times 3 \times 5 \cdots (w-1)}{2 \times 4 \times 6 \cdots w} \otimes \exp[-\beta(\Delta E - E_S - w\hbar\omega_{cf})^2 / 4E_S] , \quad (\text{III. 9})$$

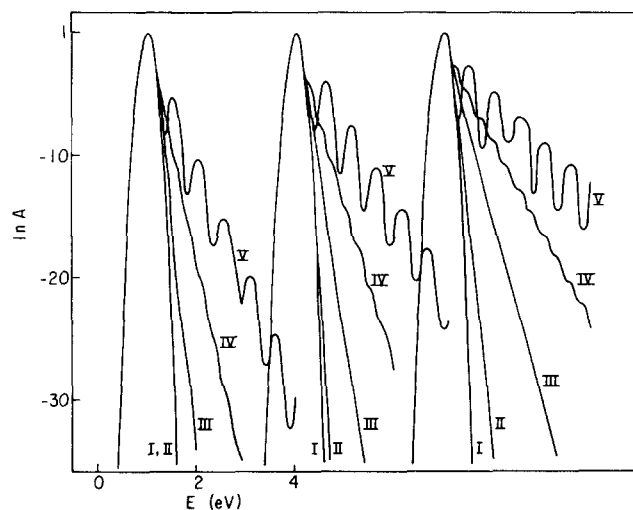


FIG. 5. Free energy plots for frequency shifts without displacement in one quantum mode. $T = 30^\circ\text{K}$. The three families of curves (from left to right) refer to $\xi = 0.1, 0.2, \text{ and } 0.4$. The origins of the latter two are shifted by 3 eV and 6 eV along the ΔE axis. Within each family, the Roman numerals refer to different frequencies of the quantum mode in the initial state: I: classical; II: $\hbar\omega_c = 206 \text{ cm}^{-1}$; III: $\hbar\omega_c = 514 \text{ cm}^{-1}$; IV: $\hbar\omega_c = 1029 \text{ cm}^{-1}$; V: $\hbar\omega_c = 2058 \text{ cm}^{-1}$.

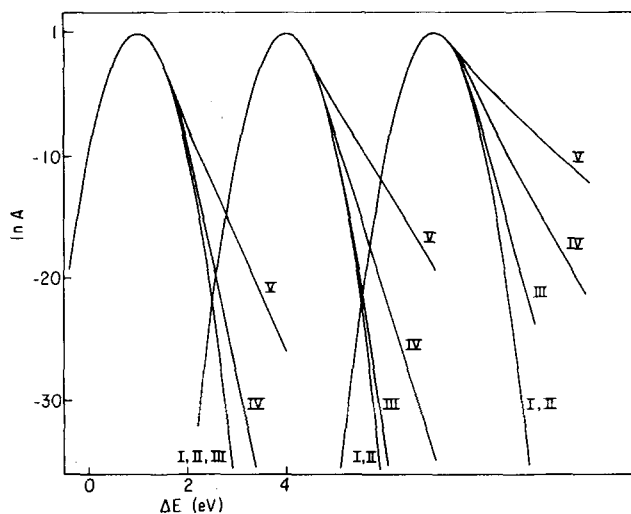


FIG. 6. Free energy plots for frequency shifts without displacement in one quantum mode. $T = 298^\circ\text{K}$. The ξ and frequency values and the arrangement of the plots are the same as in Fig. 5.

where $\overline{\Delta E}$ is the energy gap containing the difference in zero point energies of the initial and final states, i. e., $\overline{\Delta E} = \Delta E + \frac{1}{2}\hbar(\omega_{cf} - \omega_{ci})$. Equation (III. 7) shows that A is the same for positive and negative ξ . Since, furthermore, the ratio of the factorials in (III. 7) is a slowly varying function of w , the dominating factors in the free energy relationship are

$$\xi^w \exp[-\beta(\Delta E - E_s - w\hbar\omega_{cf})^2/4E_s].$$

In all cases $0 \leq |\xi| < 1$. The limiting value $|\xi| \rightarrow 1$ corresponds to complete bond breaking or establishment of a new bond. Typically $|\xi| \ll 1$, e. g., for many coordination compounds, in which the oxidized and reduced form of the metal ion differ by one charge unit, $\xi \approx 0.1 - 0.2$. In many cases ξ^w therefore decreases rapidly with increasing w , and the sum in Eq. (III. 7) should therefore converge rapidly after having passed through a maximum value for some value of ΔE . It should be noted that when $\hbar\omega_c$ is sufficiently large compared with $2(E_s k_B T)^{1/2}$, both Eqs. (III. 4) and (III. 9) predict an oscillatory relationship between $\ln A$ and ΔE . This effect is seen in Figs. 5 and 6, but most clearly at 30°K , where the Gaussian functions are narrow compared with $\hbar\omega_c$.

For distortions without displacement in N identical modes, such as a group of metal-ligand stretching modes, the Franck-Condon factors are²⁹

$$A = (\pi/\hbar^2 E_s k_B T)(1 - \xi^2)^{1/2} \exp(-\Delta_c^2/2) \sum_{w=0}^{\infty} w! [\Delta_c^2(1 - \xi)/2]^w \otimes \left| \sum_{r=0}^{w/2} [\Delta_c^2(1 - \xi)/\xi]^r / (w - 2r)! r! \right|^2 \exp[-\beta(\Delta E - E_s - w\hbar\omega_{cf})^2/4E_s]. \quad (\text{III. 14})$$

Figures 5 and 6 show free energy plots for a pure distortion in the low temperature limit [Eq. (III. 9)] for various values of ξ and $\hbar\omega_c$. The "asymmetry" of the plots is more pronounced for higher ξ and $\hbar\omega_c$, and so

$$S_{ab}^{DA}(0, w) = (1 - \xi^2)^{1/2} \xi^{w^{\dagger}} \frac{N(N+2)(N+4) \cdots (N+w^{\dagger} - 2)}{2 \times 4 \times 6 \cdots w^{\dagger}}, \quad (\text{III. 10})$$

where $w^{\dagger} = \sum_i w_i$, and provided that all the w_i 's, i. e., the vibrational quantum numbers of the various modes, are even. A particularly simple form is obtained for $N = 2$,

$$S_{ab}^{DA}(0, w) = (1 - \xi^2)^{1/2} \xi^{w^{\dagger}}. \quad (\text{III. 10}')$$

Since again the factorials are slowly varying functions of w^{\dagger} (or even a constant = 1 for $N = 2$), it is seen that the same qualitative form of the free energy plot is obtained as for a single mode, i. e., $\ln A$ goes through a maximum for increasing values of ΔE .

In most real systems undergoing a distortion, a displacement accompanies the frequency change. It is therefore necessary to consider also the full expression [Eq. (III. 5)] including both factors. This form is physically less transparent, and the qualitative behavior of the free energy plot is not immediately obvious. However, the Franck-Condon factor can be rewritten in the following way:

$$S_{ab}^{DA}(0, w) = (1 - \xi^2)^{1/2} \exp(-\Delta_c^2/2) \times (\xi/2)^w w! \left| \sum_{r=0}^{w/2} (2x)^{w-2r} / (w - 2r)! r! \right|^2. \quad (\text{III. 11})$$

It can be shown that

$$(\xi/2)^w w! \left| \sum_{r=0}^{w/2} (2x)^{w-2r} / (w - 2r)! r! \right|^2 \ll \left(\frac{\Delta_c^2(1 - \xi)}{2} \right)^w / w! \left| \sum_{r=0}^{w/2} \left(\frac{\Delta_c^2(1 - \xi)}{\xi} \right)^r w^{2r} / r! \right|^2. \quad (\text{III. 12})$$

Since $[\Delta_c^2(1 - \xi)/2][\Delta_c^2(1 - \xi)/\xi]^{-1} < 1$ for all ξ and Δ_c , $S_{ab}^{DA}(0, w)$ converges if

$$P(w) = \left| \sum_{r=0}^{w/2} w^{2r} / 2r! \right|^2 / w! \quad (\text{III. 13})$$

converges. For large w ,

$$P(w) \approx e^w \left| \sum_{r=0}^{w/2} w^{2r-w} / r! \right|^2. \quad (\text{III. 13}')$$

Since $w \geq 2r$, $P(w)$ increases substantially more slowly with increasing w than e^w . The product of $S_{ab}^{DA}(0, w)$ and the Gaussian function of w from the activation factor therefore decreases rapidly with increasing w , and the summations over w and r in Eq. (III. 14) below are convergent. $\ln A$ again goes through a maximum for increasing ΔE , the explicit expression for A being

is the expected oscillatory behavior, due to the low half-widths $2(E_s k_B T)^{1/2}$ of the Gaussian functions at this temperature. Analogous calculations were performed for higher temperatures [but still for $\beta\hbar\omega_c \ll 1$, case (a)],

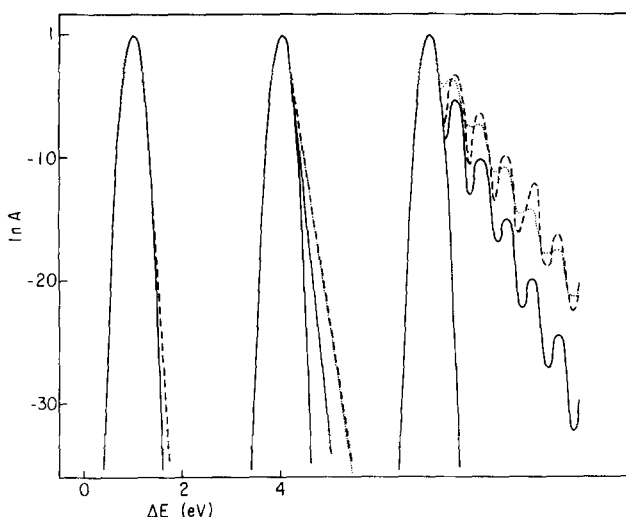


FIG. 7. Free energy plots for frequency shifts without displacement in two quantum modes. $T=30^\circ\text{K}$, and $\xi=0.2$. The three families of curves (from left to right) refer to $\hbar\omega_{c1}=206\text{ cm}^{-1}$, 514 cm^{-1} , and 2058 cm^{-1} , and the origins of the latter two are shifted by 3 eV and 6 eV along the ΔE axis. Within each family, the different lines refer to the following cases: (—) (more symmetric): classical; (—) (less symmetric): frequency shift in one mode; (···): frequency shift in two modes, for which $\hbar\omega_{c2}=0.7\hbar\omega_{c1}$; (---): frequency shift in two modes for which $\hbar\omega_{c2}=\hbar\omega_{c1}$.

and for two modes with equal and different frequencies. As expected, under these conditions the oscillatory behavior is "smoothed out," as seen for the plots with distortions in two modes in Fig. 7.

C. Effects of anharmonicities

Up to this point we have adopted the conventional approach of solid state physics⁵ utilizing the harmonic approximation both for the low-frequency solvent modes and for the high-frequency quantum modes. The harmonic approximation is definitely adequate for the solvent modes, however, for the quantum modes anharmonicity effects may considerably affect the value of the transition probability. We are interested in highly exothermic electron transfer processes where $\Delta E/\hbar\omega_{ci}$ is fairly large. It is now well known from the studies of nonradiative electronic relaxation phenomena in large

organic molecules²⁸ and in impurity centers in crystals³¹ that anharmonicity effects do drastically modify the non-radiative transition probability for a large energy gap. In what follows we shall explore the role of diagonal anharmonicity effects on ET processes.

In order to investigate this matter, the Franck-Condon factors were calculated by means of wavefunctions corresponding to Morse potentials in the initial and final states.³¹⁻³³ The general form of the potential surfaces for a single quantum mode in the initial and final states are

$$U_a(Q) = D[1 - \exp(-aQ)]^2, \\ U_b(Q) = D\{1 - \exp[-a(Q + \Delta_c)]\}^2 + \Delta E, \quad (\text{III. 15})$$

where D is the dissociation energy, Δ_c the displacement of the coordinate Q , and a the anharmonicity constant. For the sake of simplicity, it is assumed that D and a (and the vibration frequency) are the same in the two states. The total energy of the anharmonic mode is

$$E^{(w)} = \hbar\omega_c(w + \frac{1}{2}) - \frac{1}{2}\hbar\omega_c a^2(w + \frac{1}{2})^2. \quad (\text{III. 16})$$

The general form of the overlap integral for this mode between the ground vibrational level of the initial state $\bar{\chi}_{a0}$ and the w th level of the final state $\bar{\chi}_{bw}$ can be written as^{32,33}

$$\frac{\langle \bar{\chi}_{bw} | \bar{\chi}_{a0} \rangle}{\langle \bar{\chi}_{b0} | \bar{\chi}_{a0} \rangle} = (-1)^w (1 - 2w/p) \binom{p}{w}^{1/2} \sum_{\sigma=0}^w (-1)^\sigma \frac{\Gamma(p-\sigma)}{\Gamma(p)} \binom{w}{\sigma} \\ \otimes \frac{\Gamma(p+1-w)}{\Gamma(p+1-w-\sigma)} \frac{1}{2} (1 + e^{-a\Delta_c})^\sigma \quad (\text{III. 17})$$

and

$$\langle \bar{\chi}_{b0} | \bar{\chi}_{a0} \rangle = 2^p e^{(1/2)ap\Delta_c} (1 + e^{a\Delta_c})^{-p}, \quad (\text{III. 18})$$

where $p = 2a^{-2} - 1$. Rearranging Eqs. (III. 17) and (III. 18) gives for transition to the lowest vibrational levels

$$\langle \bar{\chi}_{b0} | \bar{\chi}_{a0} \rangle = [\cosh(a\Delta_c/2)]^{-p} \quad (\text{III. 19a})$$

$$\langle \bar{\chi}_{b1} | \bar{\chi}_{a0} \rangle = [\cosh(a\Delta_c/2)]^{-p} \frac{1}{4} (p-2)(1 - e^{-a\Delta_c})^2. \quad (\text{III. 19b})$$

For transition to the w th final vibrational level, the Franck-Condon factor can be written in the compact form

$$S_{ab}^{DA} \equiv \langle \bar{\chi}_{bw} | \bar{\chi}_{a0} \rangle^2 = [\cosh(a\Delta_c/2)]^{-2p} [(1 - 2w/p) \binom{p}{w}]^2 \otimes \left[\sum_{\sigma=0}^w (-1)^\sigma \left[\frac{1}{2} (1 + e^{-a\Delta_c}) \right]^\sigma \binom{p-w}{\sigma} \binom{p-1}{\sigma}^{-1} \binom{w}{\sigma} \right]^2. \quad (\text{III. 20})$$

The transition probability for this mode then becomes, for a system which involves displacement in a single anharmonic mode in the low temperature limit

$$A = (\pi/\hbar^2 E_S k_B T)^{1/2} [\cosh(a\Delta_c/2)]^{-2p} \sum_{w=0}^{\infty} [(1 - 2w/p) \binom{p}{w}]^2 \otimes \left[\sum_{\sigma=0}^w (-1)^\sigma \left[\frac{1}{2} (1 + e^{-a\Delta_c}) \right]^\sigma \binom{p-w}{\sigma} \binom{p-1}{\sigma}^{-1} \binom{w}{\sigma} \right]^2 \\ \otimes \exp\{-\beta[\Delta E - E_S - \hbar\omega_c(w + \frac{1}{2}) + \frac{1}{2}\hbar\omega_c a^2(w + \frac{1}{2})^2]\}. \quad (\text{III. 21})$$

In order to investigate the physical effect of the anharmonicity, it should first be noted that for typical mo-

lecular dissociation energies,³¹ $a \approx 0, 1$, and $p \approx 10^2$. For the hypothetical case of transitions involving the

ground vibrational levels of the quantum mode, Eq. (III. 19a), the effect of anharmonicity is to increase the value of the transition probability as compared to the harmonic value, due to an increased value of the pre-exponential Franck–Condon factor, since $[\cosh(a\Delta_c/2)]^{-2\sigma} > \exp(-\Delta_c^2/2)$ for a finite value of Δ_c . This effect can be very pronounced; for example, when $\Delta_c \approx 1-2$, the two factors are very close to each other, both being of the order of unity, whereas for $\Delta_c \approx 10$ they are about 10^{-5} for the anharmonic case and 10^{-22} for the harmonic case. The increased transition probability is again related to the decreased barrier height and width for the “tunneling” of the quantum mode, as compared with the harmonic model.

When higher vibronic levels contribute considerably to the reaction rate, the transition probability is determined not only by the numerical value of Δ_c but also by its sign. This is reflected by the factors $[\frac{1}{2}(1 + e^{-a\Delta_c})]^\sigma$ in Eq. (III. 21). Thus, when anharmonicity effects are important, one has to specify carefully whether the situation corresponds to stretching ($\Delta_c > 0$) or compression ($\Delta_c < 0$) of a quantum mode. It can be shown by inspection of Eq. (III. 21) that when excited vibrational states participate in the reaction, positive displacements ($\Delta_c > 0$) result in an increased value of A , as compared to the value A_{har} obtained from the harmonic approximation with the same value of Δ_c ; whereas for $\Delta_c < 0$, $A < A_{\text{har}}$. Thus, for the model system involving a single quantum mode, the ET transition probability can be either enhanced ($\Delta_c > 0$) or retarded ($\Delta_c < 0$) relative to the result of the harmonic model, depending on the absolute sign of Δ_c .

In the treatment of outer sphere ET reactions, one cannot get away with the simple model system involving a single displaced quantum mode, and one has to consider at least displacements in two quantum modes which correspond to the symmetrical stretching and compression of the metal–ligand bonds of the electron acceptor and of the electron donor, respectively. Furthermore, we accept that in general the displacements Δ_{c_1} and Δ_{c_2} will be of opposite signs. Since the contribution of anharmonicity effects to the exponential temperature dependent factors is considerably smaller than to the pre-exponential terms in Eq. (III. 21), the major anharmonicity effect on A originates from the vibrational overlap integrals. When Franck–Condon factors for two modes characterized by opposite signs of the displacements are incorporated in Eq. (III. 21), the anharmonicity effects will cancel to a considerable extent.

We thus expect that for a system characterized by two displacements of opposite signs in anharmonic modes, the value of A will be close to A_{har} . Cancellation of anharmonic effects by displacements of different signs may provide a rationalization for the surprisingly good agreement³⁴ obtained between experimental data for ET reactions and the theoretical data calculated within the framework of the harmonic approximation.

IV. CONCLUDING REMARKS

We have advanced a general quantum mechanical formalism for the role of quantum modes on outer sphere

ET processes. The electron donor–electron acceptor pair together with the entire polar solvent are envisioned as a “supermolecule” undergoing a nonradiative decay process. We have explicitly shown how the contributions of the quantum modes and of the “classical” solvent modes can be segregated. The ET rate constant was finally recast in the form of sums of products, where each term involves a product of a Franck–Condon vibrational overlap term for the quantum modes and a Gaussian function $\exp(-y^2/\gamma^2)$, where $y = \Delta E - E_S + (\epsilon_a^D + \epsilon_a^A) - (\epsilon_b^D + \epsilon_b^A)$ and $\gamma = 2(E_S k_B T)^{1/2}$, for the solvent polar modes. We note in passing that energy conservation is insured for each of these terms. In view of our current ignorance of the details of the potential energy surfaces for the electron donor and acceptor quantum modes, i. e., displacements of origins, frequency changes, and anharmonicity constants, we have proceeded to consider several simple model systems. We were able to explore the effects of quantum modes on the free energy relationships. Three interesting effects emerge in this context. First, the asymmetry in the free energy relation resulting in the slow decrease of $\ln A$ (and consequently of $\ln k$) with increasing ΔE for strongly exothermic ET processes, characterized by large values of $\hbar\omega_c$ and of Δ_c provides a rationalization for the experimental observation of an “activationless” region for exothermic ET reactions involving large electronically excited organic molecules²² and radical ion recombination.²⁴ These systems that were experimentally studied involve high-frequency intramolecular modes which are distorted between different valence states. Thus the conditions for attaining a flat portion of the $\ln k$ vs ΔE dependence for $-\Delta E < 0$ are met. Second, we have observed the pronounced isotope effects originating from the role of quantum modes on the ET transition probability. This effect bears a close analogy to the deuterium isotope effects exhibited in nonradiative electronic relaxation processes in large molecules¹; however, in the case of ET processes, both normal and inverse isotope effects can be exhibited, whereas in the case of electronic relaxation the common state of affairs involves a normal deuterium isotope effect. Third, for the case of a high-frequency mode $\hbar\omega_c \approx 2000-3000 \text{ cm}^{-1}$ undergoing either displacement or frequency change, we have observed an oscillatory dependence in the free energy relationship at low temperature, the spacing between the maxima being $\sim \hbar\omega_c$. This interesting quantum effect is analogous to the vibrational structure in optical spectroscopy.

If we consider for the moment an optical transition between the states $|av\rangle$ and $|bw\rangle$, Eq. (I. 1), the radiative transition probability $\Gamma(h\nu)$ (for a dipole allowed transition) at the photon energy $h\nu$ is⁵

$$\Gamma(h\nu) = \frac{2\pi}{\hbar} |\langle \psi_a | \mu | \psi_b \rangle|^2 Z^{-1} \sum_v \sum_w \exp(\beta E_{av}) \times |\langle \chi_{av} | \chi_{bw} \rangle|^2 \otimes \delta(E_{av} - E_{bw} + \Delta E \pm h\nu), \quad (\text{IV. 1})$$

where μ is the electronic transition moment, handled within the framework of the Condon approximation, while the minus and the plus signs in the delta function refer to photon emission and absorption, respectively. As we are interested in the case $\Delta E > 0$, emission processes

are relevant. Comparing Eq. (IV.1) with the nuclear contribution Eq. (I.6) to the ET rate, two points become apparent. First, we note that $\Gamma(o)/|\langle\psi_a|\mu|\psi_b\rangle|^2 = A$ and, as we have already stated, the nonradiative ET process is formally analogous to the radiative emission process at zero energy. Second, and most important, the functional dependence of $\Gamma(h\nu)$ [or rather of $\Gamma(\Delta E - h\nu)$] on $(\Delta E - h\nu)$ for the emission process is identical to the dependence of A on ΔE . Thus, the optical line shape for emission is formally analogous to the free energy relationship for ET, provided that the variation of Γ with $\Delta E - h\nu$ in the former case is replaced by the variation of A with changing ΔE in the latter case. On the basis of this formal analogy we conclude that monitoring the free energy relationship for a class of "closely related" ET reactions can be considered as an experiment in "chemical type spectroscopy" where the photon energy in an ordinary spectroscopic measurement is replaced by the variation of the free energy. Pursuing this interesting analogy between conventional optical spectroscopy and chemical type spectroscopy, we realize that the optical line shape of a large molecule in solution can be handled by considering Eq. (IV.1), incorporating both solvent (low frequency, but not necessarily polar) modes and the intramolecular quantum modes and adopting the treatment outlined in Sec. II. of the present paper. The vibrational structure of optical electronic transitions in large organic molecules in solution exhibit broad bands, exhibiting vibrational progressions which correspond to high-frequency totally symmetric modes, which are displaced between the two electronic configurations. The oscillatory dependence of A on ΔE at low temperatures (for high $\hbar\omega_c$) reflects the vibrational structure due to a quantum mode in the free energy relationship. What remains now is to establish quantitative conditions for the observation of the "oscillatory" behavior in the free energy relationship. From the general structure of Eq. (II.13) we assert that structure in the A vs ΔE curve will be exhibited provided that the spacing between the quantum states will exceed the width $\gamma = 2(E_s k_B T)^{1/2}$ of the Gaussian term, whereupon

$$\epsilon_a^D + \epsilon_a^A - \epsilon_b^D - \epsilon_b^A > 2(E_s k_B T)^{1/2}. \quad (\text{IV.2})$$

For reasonable values of $E_s \approx 1$ eV, $\gamma = 800$ cm⁻¹ at 30 °K and $\gamma = 2560$ cm⁻¹ at 300 °K, so that even for a single active quantum mode all structure will be smoothed out at room temperature. For real systems this structure will be further blurred by frequency shifts and by displacements of several modes characterized by different frequencies. Nevertheless, the predicted oscillatory behavior of the free energy relationship may be amenable to experimental observation for some selected systems at sufficiently low temperatures (~ 4 °K). This effect provides, in addition to the temperature dependence of the activation energy,⁴ a new and interesting quantum phenomenon, which may yield direct information concerning the nature of quantum modes participating in ET processes.

ACKNOWLEDGMENT

We are grateful to Mr. Niels S ndergaard for performing the numerical calculations.

*Permanent address.

- ¹(a) M. Bixon and J. Jortner, *J. Chem. Phys.* **48**, 715 (1968); (b) M. Bixon and J. Jortner, *J. Chem. Phys.* **50**, 3284 (1969); (c) J. Jortner and S. Mukamel, in *The World of Quantum Chemistry*, edited by G. R. Daudel and B. Pullman (Reidel, Dordrecht and Boston, 1974), p. 145; (d) R. Englman and J. Jortner, *Mol. Phys.* **18**, 145 (1970); (e) W. M. Gelbart, K. G. Spears, K. F. Freed, S. A. Rice, and J. Jortner, *Chem. Phys. Lett.* **6**, 345 (1970).
- ²S. Mukamel and J. Jortner, *J. Chem. Phys.* **60**, 4760 (1974).
- ³F. H. Mies and M. Krauss, *J. Chem. Phys.* **45**, 4455 (1966).
- ⁴N. R. Kestner, J. Logan, and J. Jortner, *J. Phys. Chem.* **78**, 2148 (1974).
- ⁵(a) R. Kubo and Y. Toyozawa, *Prog. Theor. Phys.* **13**, 161 (1955); (b) T. Holstein, *Ann. Phys.* **8**, 325 (1959).
- ⁶V. G. Levich, *Adv. Electrochem. Electrochem. Eng.* **4**, 249 (1966).
- ⁷R. Saxton, *Proc. R. Soc. London Ser. A* **213**, 473 (1952).
- ⁸R. R. Dogonadze, in *Reactions of Molecules at Electrodes*, edited by N. S. Hush (Wiley-Interscience, London, 1971).
- ⁹R. A. Marcus, *J. Chem. Phys.* **24**, 966 (1956).
- ¹⁰W. L. Reynolds and R. W. Lumry, *Mechanisms of Electron Transfer* (Ronald, New York, 1966).
- ¹¹F. Basolo and R. G. Pearson, *Mechanisms of Inorganic Reactions* (Wiley, New York, 1967), 2nd ed.
- ¹²Yu. I. Kharkats, *Elektrokhimiya* **9**, 881 (1973).
- ¹³Yu. I. Kharkats, *Elektrokhimiya* **10**, 612 (1974).
- ¹⁴R. A. Marcus, *Discuss. Faraday Soc.* **29**, 21 (1960).
- ¹⁵M. A. Vorotyntsev, R. R. Dogonadze, and A. M. Kuznetsov, *Phys. Status Solidi* **54**, 125 (1972).
- ¹⁶M. A. Vorotyntsev, R. R. Dogonadze and A. M. Kuznetsov, *Phys. Status Solidi* **54**, 425 (1972).
- ¹⁷R. R. Dogonadze, J. Ulstrup, and Yu. I. Kharkats, *J. Chem. Soc. Faraday Trans.* **68**, 744 (1972).
- ¹⁸E. D. German and R. R. Dogonadze, *J. Res. Inst. Catal. Hokkaido Univ.* **20**, 34 (1972).
- ¹⁹E. D. German and R. R. Dogonadze, *Int. J. Chem. Kinet.* **6**, 457 (1974).
- ²⁰W. Schmickler, *Proc. 25th ISE Meeting, Brighton, 1974*, p. 79.
- ²¹S. Efrima and M. Bixon, *Chem. Phys. Lett.* **25**, 34 (1974).
- ²²D. Rehm and A. Weller, *Israel J. Chem.* **8**, 259 (1970).
- ²³S. F. Fischer, *Proc. 25th ISE Meeting, Brighton, 1974*, p. 63.
- ²⁴R. P. Van Duyne, *Proc. 25th ISE Meeting, Brighton, 1974*, p. 63.
- ²⁵V. G. Levich, E. D. German, R. R. Dogonadze, A. M. Kuznetsov, and Yu. I. Kharkats, *Electrochim. Acta* **15**, 353 (1970).
- ²⁶M. D. Glick, J. M. Kuszaj, and J. F. Endicott, *J. Am. Chem. Soc.* **95**, 5097 (1973).
- ²⁷K. F. Freed and J. Jortner, *J. Chem. Phys.* **52**, 6272 (1970).
- ²⁸A. Nitzan and J. Jortner, *Theor. Chim. Acta* **30**, 217 (1973).
- ²⁹W. Siebrand, *J. Chem. Phys.* **46**, 440 (1967).
- ³⁰W. Siebrand, *J. Chem. Phys.* **47**, 2411 (1967).
- ³¹M. D. Sturge, *Phys. Rev. B* **8**, 6 (1973).
- ³²P. A. Fraser and W. R. Jarman, *Proc. Phys. Soc. London Sect. A* **66**, 1145 (1953).
- ³³P. A. Fraser and W. R. Jarman, *Proc. Phys. Soc. London Sect. A* **66**, 1153 (1953).
- ³⁴J. M. Hale, in *Reactions of Molecules at Electrodes*, edited by N. S. Hush (Wiley-Interscience, London, 1971).